Supplemental material

Gilmore-Hall et al., https://doi.org/10.1083/jcb.201709028

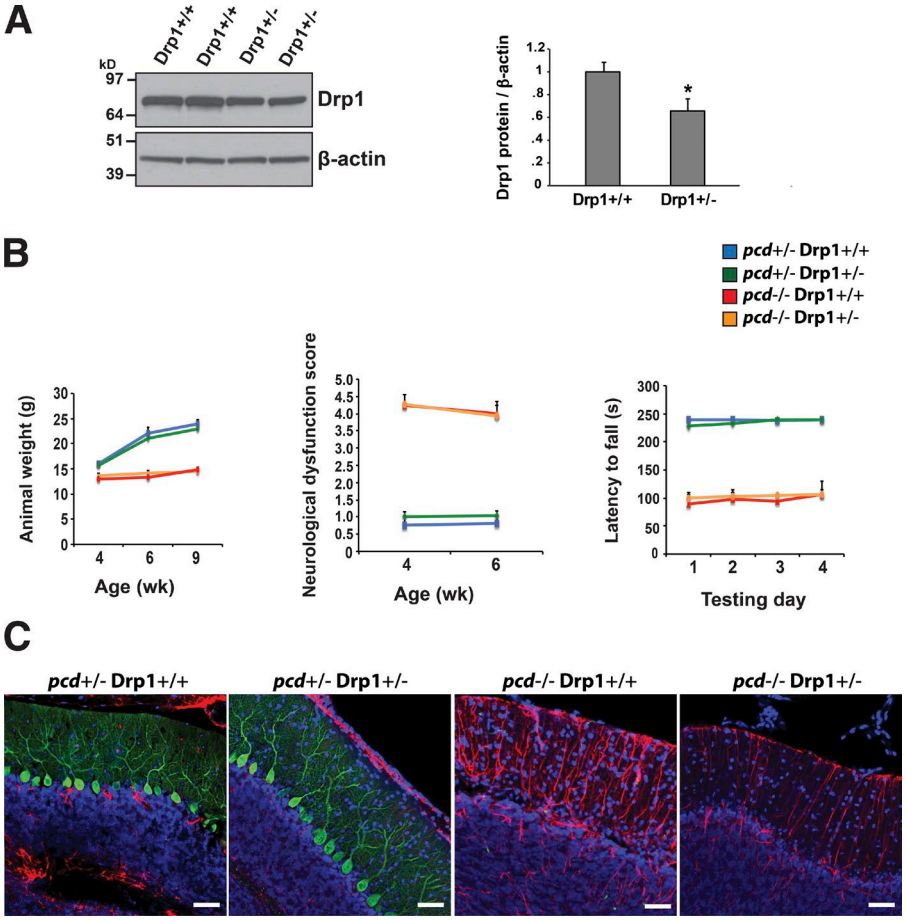

Figure S1. **Dosage reduction of Drp1 does not rescue *pcd* phenotypes. (A)** Immunoblot analysis of Drp1 protein expression in cerebellar protein lysates from *Drp1*$^{+/+}$ or *Drp1*$^{+/-}$ mice, with densitometry analysis of CCP1 expression relative to β-actin expression for $n = 3$ replicates, shown on right. *t* test: $P < 0.05$. **(B)** Phenotype and behavioral analysis of the indicated *pcd* × *Drp1* genotypes including weight, neurological examination, and accelerating rotarod. Reduced Drp1 dosage did not affect any of these readouts in *pcd* homozygous mice. **(C)** Immunohistochemistry of cerebellar sections from 3-mo-old *pcd* × *Drp1* mice reveals no benefit from reduced Drp1 dosage in *pcd* homozygous mice. Green indicates calbindin, red indicates GFAP, and blue indicates Hoechst 33342. Bars, 25 µm. Error bars are SEM.

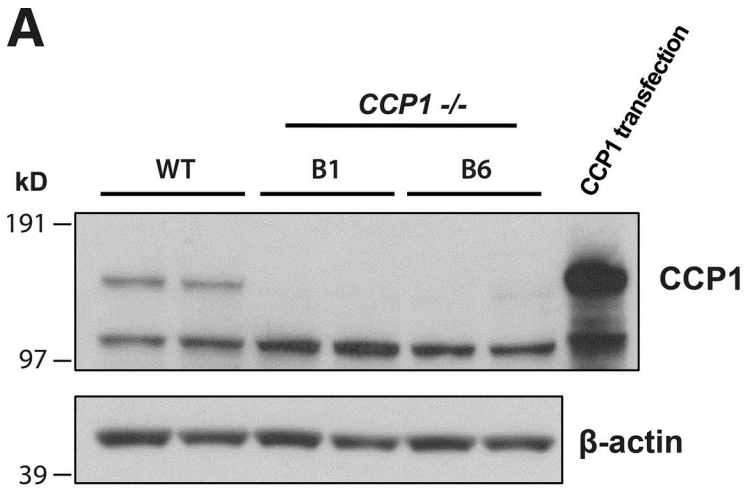

B

CCP1-KO cell line	Mutations
B1	1 bp insertion; 207 bp insertion
B6	1 bp insertion; 3 bp deletion

Figure S2. **Validation of CCP1 knockout RPE1 cell lines. (A)** Immunoblot analysis of CCP1 expression in WT RPE1 cells and in two different CCP1 null RPE1 cell lines confirms absence of CCP1 protein expression. The CCP1-transfected HEK293 cell protein lysates served as a positive control for CCP1 detection. **(B)** Results of sequencing of CCP1 genes in CRISPR/Cas9 targeted null cell lines reveal the mutational basis of each knockout cell line.

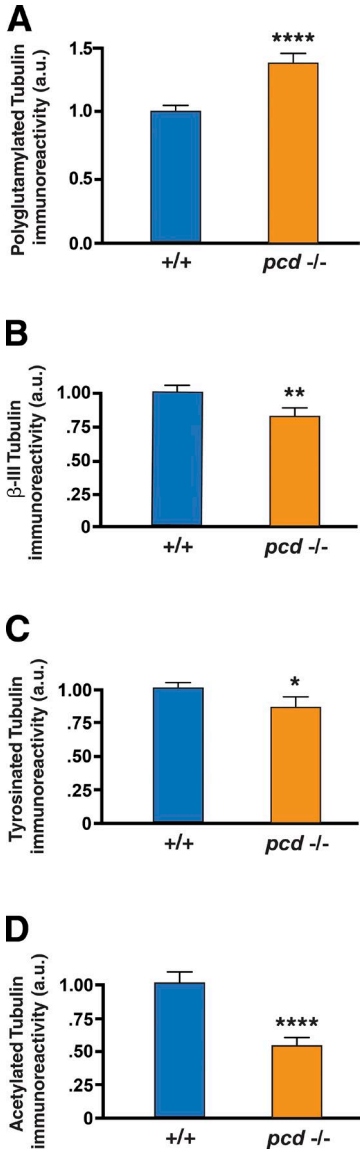

Figure S3. **Loss of CCP1 results in significant changes in the levels of tubulin PTMs. (A)** Quantification of polyglutamylated tubulin immunoreactivity in Purkinje cell neurons of 23-d-old WT (+/+) littermate control mice and *pcd* homozygous (−/−) mice from Fig. 7 C. Immunoreactivity for +/+ mice was arbitrarily set to 1. n = 3 mice per genotype; $n \geq 60$ Purkinje cells per genotype. **(B)** Quantification of βIII-tubulin immunoreactivity in Purkinje cell neurons of 23-d-old WT (+/+) littermate control mice and *pcd* homozygous (−/−) mice from Fig. 4 D. Immunoreactivity for +/+ mice was arbitrarily set to 1. n = 3 mice per genotype; $n \geq 30$ Purkinje cells per genotype. **(C)** Quantification of tyrosinated tubulin immunoreactivity in Purkinje cell neurons of 23-d-old WT (+/+) littermate control mice and *pcd* homozygous (−/−) mice from Fig. 7 E. Immunoreactivity for +/+ mice was arbitrarily set to 1. n = 3 mice per genotype; $n \geq 35$ Purkinje cells per genotype. **(D)** Quantification of acetylated tubulin immunoreactivity in Purkinje cell neurons of 23-d-old WT (+/+) littermate control mice and *pcd* homozygous (−/−) mice from Fig. 7 F. Immunoreactivity for +/+ mice was arbitrarily set to 1. n = 3 mice per genotype; $n \geq 25$ Purkinje cells per genotype. Two-tailed t test: *, $P < 0.05$; **, $P < 0.01$; ****, $P < 0.0001$. Error bars are SEM.

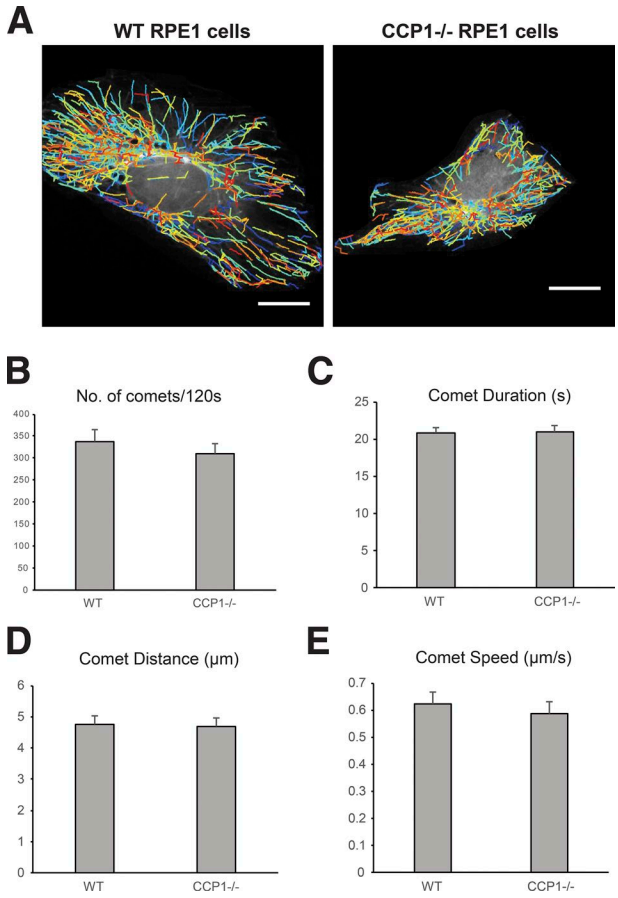

Figure S4. **The Eb1-GFP comet assay indicates normal nascent MT formation in CCP1 null cells. (A)** Stacked tracks from 120 s of live imaging of Eb1-GFP in either WT or *nna1*Δ RPE1 cells. Colors represent order of tracks in time lapse; blue indicates early, and red indicates late. Bars, 20 µm. **(B–E)** Quantification analysis using ImageJ-based Trackmate to determine the average number of comets per 120 s (B), mean comet duration (C), mean comet displacement (D), and mean comet speed (E). All of these parameters were similar between WT cells and CCP1$^{-/-}$ cells. *n* = 25–27 cells per genotype. Error bars are SEM.

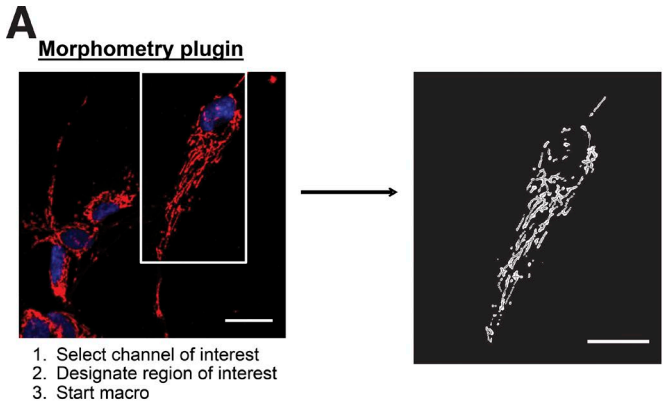

file	perimeter	Form factor	Aspect ratio	awff	length
Image 26.jpg	57	2.7685	3.0086	9.6641	41.8

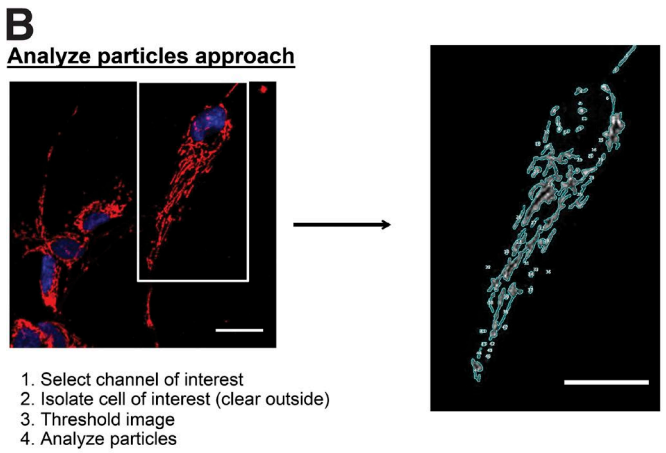

Mitochondria	Area	Mean int	Perimeter	Major axis	Minor axis	Major/minor
1	367	168.7248	127.58074	62.50805	7.4755	8.361721624
2	122	145.2623	43.69848	17.22056	9.02034	1.909081032
3	2529	168.34559	448.75945	106.72321	30.17172	3.537193438
4	251	141.80478	80.3259	27.11714	11.78528	2.300933028
5	22	81.77273	18.97056	6.46376	4.33359	1.491548578
6	43	105.60465	23.2132	8.1549	6.71367	1.214670962
7	227	148.96035	64.08326	26.09386	11.07638	2.355811195

Figure S5. **Algorithms employed to quantify mitochondrial morphology characteristics and detect mitochondrial fragmentation. (A)** We employed an ImageJ-based morphometry algorithm to calculate mitochondrial perimeter, form factor, area-weighted form factor (awff), and aspect ratio in each individual retinal pigmented epithelial cell immunostained with Tomm20 (red) and Hoechst 33342 (blue). **(B)** We employed an ImageJ-based particle analysis algorithm to measure the area of each mitochondrion in an individual retinal pigmented epithelial cell immunostained with Tomm20 (red) and Hoechst 33342 (blue). We classified a cell as consisting of fragmented mitochondria when >50% of the mitochondria exhibited an area value <200. Bars, 20 µm.